

PLANAR CRACK PROPAGATION: A NUMERICAL INVESTIGATION

Nadjime Pindra

Université de Lomé, Département de Mathématiques, 1515 Lomé, Togo

ABSTRACT

The propagation of a crack at a weak disordered interface between two elastic plates is investigated numerically. The fracture front evolution is described as the depinning of an elastic line in a random field of toughness. The relevance of this approach is critically tested by comparing the roughness front properties, the statistics of the local avalanches and the crack velocity distribution with recent experimental results. Our simulations capture the main features of the fracture front evolution, even though a few experimental findings are not consistent with the behavior of an elastic line close to the depinning transition. Possible improvements of the model are discussed. Finally, the average avalanche shape and the time asymmetry of the fracture front dynamics is investigated numerically so that the comparison with experiments can be pushed further in future studies.

Keywords: Heterogeneous materials, Dynamic cracks, Effective resistance.

1. INTRODUCTION

Understanding the failure properties of heterogeneous materials has driven a large research effort these last decades. Important progresses have been achieved using, and sometimes combining, complementary concepts issued from classical fracture mechanics and equilibrium physics of disordered interfaces [1, 2]. The broad interest for these questions is motivated by two important challenges: (i) understanding the role of the microstructure of materials on their failure properties is a prerequisite to make reliable predictions on the resistance and lifetime of structures. Classical fracture mechanics that describes crack propagation in homogeneous elastic media is unable to capture various aspects of the failure of materials, like the intermittent dynamics of cracks [3–5] or the scale invariant roughening of fracture surfaces [1, 6–8], but also to make predictions on the actual value of the resistance or fracture energy of a given material. Integrating the effect of material microstructure and microscale heterogeneity is the key to overcome these difficulties and open the door to the rational design of materials with improved toughness. (ii) From a broader perspective, crack propagation in disordered materials has been shown to exhibit scaling laws and universality.

In a first section, we describe the model used in our study as well as the numerical approach for the resolution of the equation of motion of the crack. In a second part, we present the main predictions of our model and confront them with the experimental studies [16, 19]. In the third part, we go beyond the experimental results reported in the literature, and make predictions on the geometry of the avalanches as well as the time-reversal properties of the crack evolution. Finally, we discuss the relevance of the depinning model to describe material failure as well as the limitations of this approach.

2. MODEL AND METHOD

2.1 Equation of motion of the crack

The geometry of the fracture test investigated in this study is inspired by the experiments [16, 19] that is presented schematically in Figure 1a. An interfacial crack propagates between two elastic plates that are separated at a constant opening rate $\frac{d\delta}{dt}$. We assume here that all the characteristic length scales of the sample (crack length, plate thickness...) are much larger than both the perturbations along the crack front and the characteristic size of the heterogeneities.

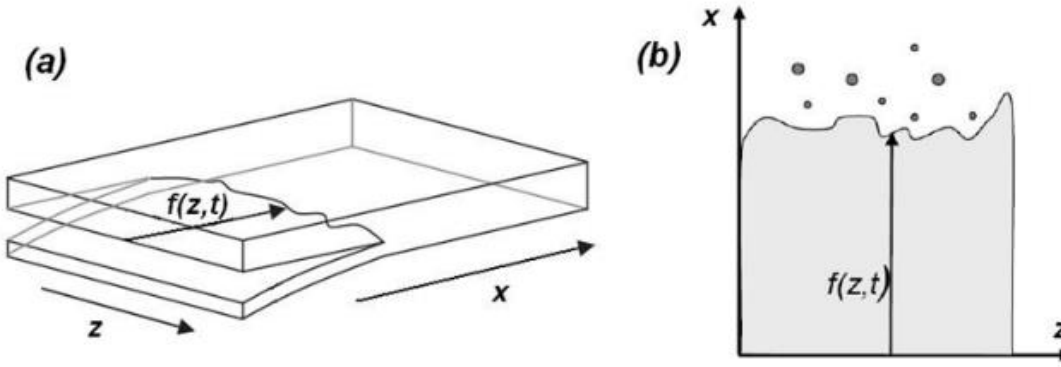


Figure 1. Geometry of the fracturing system: (a) Sketch of the experimental fracture test where an interfacial crack is made propagate at the weak interface between two elastic plates; (b) Schematic view of the heterogeneous interface where the crack front deforms under the effect of heterogeneities.

The problem of planar crack propagation within a 3D brittle solid can be reduced to a 2D problem where an interface, the crack front, is driven within a plane with heterogeneous field of toughness, as represented on Figure 1(b) [13]. The equation of motion of this line can be obtained by (i) calculating the local driving force, i.e. the elastic energy release rate $G(z)$ that applies along the crack front [15], and (ii) introducing the resistance to the front motion or fracture energy $Gc(x, z)$ at the mesoscopic scale that we will describe in the following by a random field taken in a Gaussian distribution with mean value

$\langle Gc \rangle$ and standard deviation δGc .

One obtains the following equation of motion:

$$\frac{1}{\mu} \frac{\partial f}{\partial t} = G(z, t) - Gc(z, x = f(z, t)) \quad (1)$$

Where μ represents the mobility of the front. The local driving force can be separated in three contributions [15, 28].

$$G(z, t) = G_0 + k(v_m - \dot{f}(z, t)) + \frac{G_0}{\pi} \int_{-\infty}^{+\infty} \frac{f(z') - f(z)}{(z' - z)^2} dz' \quad (2)$$

The Eqs. (1) and (2) provide a powerful tool to predict the evolution of crack fronts. Let us note that the very same equation is involved in various physical situations where an interface is driven in a medium with defects or impurities, and is known to give rise to the so-called depinning transition: the front is pinned by the heterogeneities of the media and remains stable up to some critical value G_c of the external driving force.

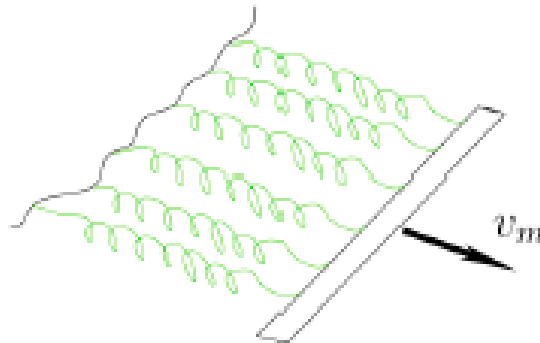


Figure 2. Elastic springs connected.

Model used for describing the loading conditions and fracture test geometry under imposed displacement: the crack front is driven by elastic springs connected to a rigid bar with stiffness and velocity v_m fixed by the geometrical parameters of the test and the material Young's modulus.

2.2 Numerical method of resolution

The crack front position is discretized over Nz points with position $z_i = Lz \times i/Nz$ for $1 \leq i \leq Nz$ where Lz is the front length along the z -axis. As a result, at a given time t , front position is represented by the Nz points $f(t) = \{f_1(t), f_2(t), \dots, f_{Nz}(t)\}$.

We impose periodic boundary conditions along the z -axis parallel to the crack front, so that a front of $2Nz$ points with $f_{BC} = \{f_{Nz/2+1}, \dots, f_{Nz}, f_1, \dots, f_{Nz}, f_1, \dots, f_{Nz/2}\}$ is actually considered. Using this discretization, the equation of motion (Eq. (1)) leads to Nz equations:

$$f_i(t + \delta t) = f_i(t) + [G_i(f_1(t) \dots f_{Nz}(t)) - G_c(z_i, f_i(t))] \times \delta t \quad (3)$$

With $1 \leq i \leq Nz$. Using a matricial form of these discretized equations and the integrals $\frac{G_0}{\pi} \int_{-\infty}^{+\infty} \frac{f(z') - f_i}{(z' - z_i)^2} dz'$

The evolution of the crack front is predicted incrementally by starting from a straight crack front at time $t = 0$ and then computing $f(t + \delta t)$ from the geometry $f(t)$ of the front at time t . Indeed, according to our explicit scheme, $f(t)$ is sufficient to compute the driving force $G(z_i)$ and the resistance $G_c(z_i, f_i)$ involved in the right-hand term of the discretized equation of motion of Eq.(3), and so to deduce $f(t + \delta t)$. We calculate the front position over a large number of time steps (typically a few millions) on a propagation distance of about one hundred heterogeneity size ξ along the x -axis. The large number of time steps ensure convergence of our numerical scheme. However, we keep only a few percent of this profiles separated by time step Δt . Δt is small enough to ensure that the front spent at least one time step on each pixel of the grid, as in the experimental conditions. The transient regime where the front geometry keeps memory of the initial straight condition is removed for the following analysis. Typically, this zone extends over a few tenths of heterogeneities size ξ along the x -direction.

2.3 Statistics of pinning and depinning clusters

The local dynamics of the fracture front is made of pinning and depinning phases, i.e. of long phases of arrest followed by abrupt motions of some portion of the front to another pinned configuration. To study both regimes, we apply the procedure proposed in Ref. [16]. We start from the waiting time matrix defined in Sec. II B that provides the time spent by the crack front on each pixel of the grid. The inverse of the waiting time matrix defines then the velocity matrix V .

In the following, we focus on the slowest driving velocity $v_m = 0.005 \xi \cdot s^{-1}$, and define depinning avalanches as domains of connected pixels for which the local velocity is greater than the threshold $C < v >$ are identified. These zones appear clearly on the depinning threshold velocity matrix. Each of these avalanches is characterized by several quantities: their width l_z along the crack front direction, their thickness l_x along the propagation direction and their size S corresponding to the total area of the cluster, the statistics of which is used here to quantify the intermittent crack dynamics and test the relevance of the theoretical approach proposed here. Similarly, the pinning clusters are defined as domains of connected pixels for which the local velocity is lower than the threshold $C < v >$.

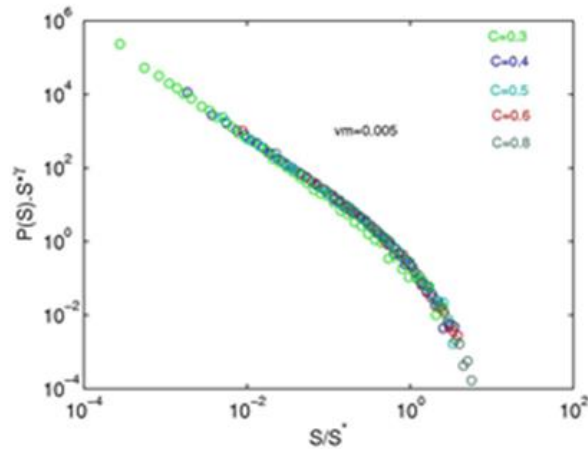


Figure 3. Avalanche size distribution after normalization

We define avalanches as areas of surface S of the interface where the local velocity of the front is greater than a threshold value C . In Figure 3., the size distribution of these avalanches is represented for different threshold values C . It follows the following law:

$$P(S) \sim S^\gamma \exp(-S/S^*) \tag{3}$$

After normalization of the curves by the quantity $S^*(c)$, we obtain the evolution given in Figure 4b, characterized by the exponent $\gamma \sim 1.6$ in good agreement with the experiments [6].

Figure 4. shows the average shape of depinning clusters for various levels of the threshold velocity C . All curves collapse on a single asymmetric shape, indicating a smaller extent of the depinning clusters in the forward than the backward direction. This observation is signature of the irreversible nature of the micro instabilities into play during the crack front evolution. This analysis shows that beyond the scaling of quantities such as cluster area or extension along some peculiar direction, their actual shape provides a very rich information on the process into play [20].

2.4 Cluster morphology

We go now beyond the statistics of local jumps of the front, and investigate the shape of both pinning and de-pinning avalanches. The morphology of these avalanches is investigated from the waiting time matrix, following the procedure described in [19]. Their typical lengths l_x and l_z along the propagation and the crack front direction respectively are defined from the maximum extent of the pinning and depinning clusters along these directions.

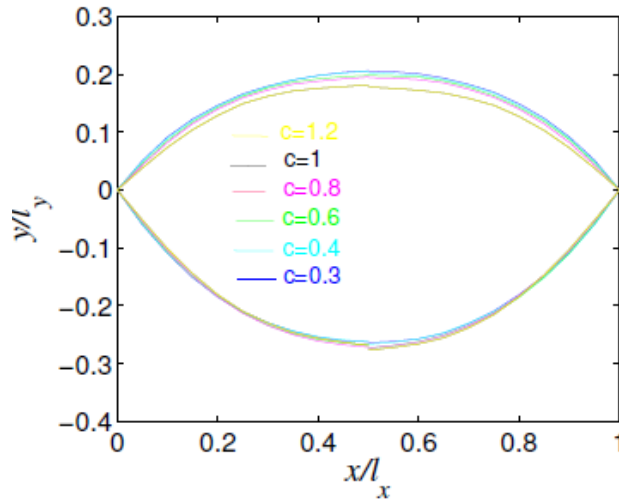


Figure 4. Average shape of the depinning cluster for various threshold C . Note the asymmetry of the clusters, signature of the asymmetry of the crack propagation process through avalanches observed in disordered materials.

Figure 4. shows the average shape of depinning clusters for various levels of the threshold velocity C . All curves collapse on a single asymmetric shape, indicating a smaller extent of the depinning clusters in the forward than the backward direction. This observation is signature of the irreversible nature of the micro instabilities into play during the crack front evolution. This analysis shows that beyond the scaling of quantities such as cluster area or extension along some peculiar direction, their actual shape provides a very rich information on the process into play [20].

2.5 Irreversibility of the motion of the front

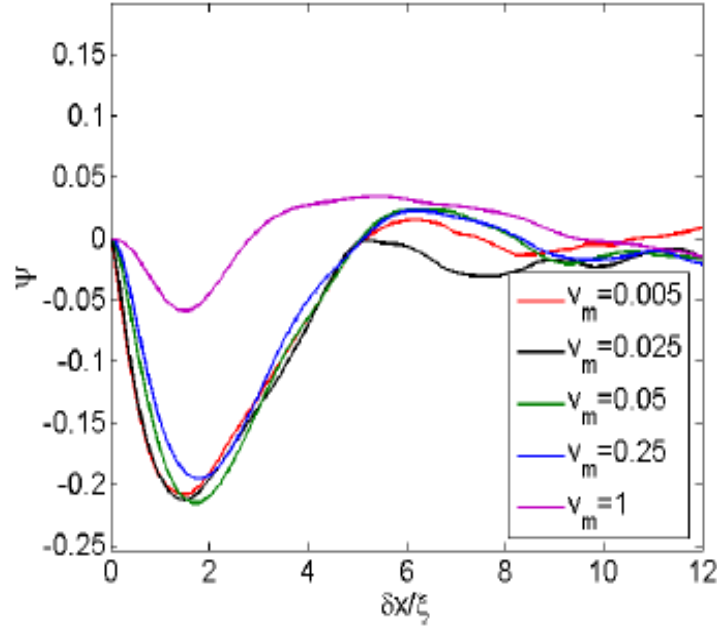


Figure 5. Correlation ψ of various imposed average velocity.

To check the asymmetry shape in previous section, we calculated the correlation function of the velocity field (Eq. (19)) for various imposed average velocity, which is not invariant under the transformation $\tau \rightarrow -\tau$.

$$\psi(\tau) = \frac{\langle (v(t)^3 v(t+\tau) - v(t)v(t+\tau)^3) \rangle_t}{\sigma^4}$$

Figure 5. shows a signature of the irreversibility of the motion of the front on the statistical avalanche. We observe a temporel asymmetry for lower propagation velocities. For the highest velocity, the correlation function is zero.

3. DISCUSSIONS

This study represents a critical test of the relevance of the equation of motion derived from Linear Elastic Fracture mechanics to rather complex materials, i.e. a weak sandblasted interface between two Plexiglas plates. Here, we show that this approach is rather well adapted to describe the main features of the intermittent dynamics of cracks in disordered media, although some predictions derived from the depinning model are not compatible with the experimental findings [3, 19]. The derivation of the model is based on several assumptions that can explained such a discrepancy: (i) the evolution equation for the crack is derived from LEFM with quasi-static conditions, i.e. in the limit of small crack growth velocities. The intermittent dynamics of crack fronts in disordered media irremediably involves instabilities, and o rapid jumps of the front from a stable position to another. (ii) The dependence of the Plexiglass properties with the loading rate or crack growth velocity has been neglected here. Viscoelastic effects or crack velocity dependent fracture energy could affect the dynamics as predicted by our model based on rate independent response of the material; (iii) we have assumed that despite the presence of various dissipated processes at the crack tip, its motion is described at the microscopic scale by a damped dynamics equation where local velocity is proportional to the difference between the local values of the driving force and the fracture energy. The characterization of the actual propagation law at the small scale is still an open question.

4. CONCLUSION

To conclude, we show here that depinning models can be used as a sound basis to predict crack properties in disordered brittle media. The few discrepancies with some of the experimental findings suggest however that a few ingredients are missing in the theoretical approach proposed in this study. Back and forth between experiments and theory on the statistical characterization of the crack evolution might help to identify these mechanisms, to that the proposed model can be enriched and improved in order to describe quantitatively the full statistics of cracks in disordered materials. Finally, our model is used to make theoretical predictions on the cluster geometry that hopefully will be tested in future experimental studies.

5. REFERENCES

- [1] M. J. Alava, P. K. Nukala, and S. Zapperi, *Adv. Phys.* 55, 349 (2006).
- [2] V. Lazarus and J. B. Leblond, *J. Mech. Phys. Solids* 46 489 (1998).
- [3] K. J. Maløy and J. Schmittbuhl, *Phys. Rev. Lett.* 87, 05502 (2001).
- [4] S. Santucci, L. Vanel, and S. Ciliberto, *Phys. Rev. Lett.* 93, 095505 (2004).
- [5] D. Bonamy, *J. Phys. D: Appl. Phys.* 42, 214014 (2009).
- [6] E. Bouchaud, G. Lapasset, and J. Planès, *Europhys. Lett.* 13, 73 (1990).
- [7] K. J. Maløy, A. Hansen, E. L. Hinrichsen, and S. Roux, *Phys. Rev. Lett.* 68, 213 (1992).
- [8] L. Ponson, D. Bonamy, and E. Bouchaud, *Phys. Rev. Lett.* 96, 035506 (2006).
- [9] E. Rolley and C. Guthmann, *Phys. Rev. Lett.* 98, 166105 (2007).
- [10] P. J. Metaxas, J. P. Jamet, A. Mougou, M. Cormier, *Phys. Rev. Lett.* 99, 217208 (2007).
- [11] P. Moretti, M. C. Miguel, M. Zaiser, and S. Zapperi, *Phys. Rev. B* 69, 214103 (2004).
- [12] S. Roux and H. Herrmann, *Statistical Models for the Fracture of Disordered Media* (Elsevier, 1990).
- [13] J. Schmittbuhl, S. Roux, J. P. Vilotte, and K. J. Maløy, *Phys. Rev. Lett.* 74, 1787 (1995).
- [14] J. P. Bouchaud, E. Bouchaud, G. Lapasset, and J. Planès, *Phys. Rev. Lett.* 71, 2240 (1993).
- [15] D. Bonamy, S. Santucci, and L. Ponson, *Phys. Rev. Lett.* 101, 045501 (2008).
- [16] S. Santucci, M. Grob, R. Toussaint, J. Schmittbuhl, A. Hansen, and K. J. Maløy, *EPL* 92, 44001 (2010).
- [17] J. Koivisto, J. Rosti, and M. J. Alava, *Phys. Rev. Lett.* 99, 145504 (2007).
- [18] L. Ponson, *Phys. Rev. Lett.* 103, 055501 (2009).
- [19] K. T. Kallakstad, R. Toussaint, S. Santucci, J. Schmittbuhl, and K. J. Maløy, *Phys. Rev. E* 83, 046108 (2011).
- [20] S. Papanikolaou, F. Bohn, R. L. Sommer, G. Durin, S. Zapperi, and J. P. Sethna, *Nature Phys.* 7, 316 (2011).
- [21] J. P. Sethna, K. A. Dahmen, and C. R. Myers, *Nature*